QEPAS based detection of broadband absorbing molecules using a widely tunable, cw quantum cascade laser at 8.4 μm.

Rafal Lewicki, Gerard Wysocki*, Anatoliy A. Kosterev, and Frank. K. Tittel.

Rice Quantum Institute, Rice University, 6100 Main St., Houston, TX 77005, USA
**Corresponding author: gerardw@rice.edu*

Abstract: Detection of molecules with wide unresolved rotational-vibrational absorption bands is demonstrated by using Quartz Enhanced Photoacoustic Spectroscopy and an amplitude modulated, high power, thermoelectrically cooled quantum cascade laser operating at 8.4 μm in an external cavity configuration. The laser source exhibits single frequency tuning of 135 cm^{-1} with a maximum optical output power of 50 mW. For trace-gas detection of Freon 125 (pentafluoroethane) at 1208.62 cm^{-1} a normalized noise equivalent absorption coefficient of NNEA=2.64×10^{-9} $cm^{-1}\cdot W/Hz^{1/2}$ was obtained. Noise equivalent sensitivity at ppbv level as well as spectroscopic chemical analysis of a mixture of two broadband absorbers (Freon 125 and acetone) with overlapping absorption spectra were demonstrated.

©2007 Optical Society of America

OCIS codes: (300.6390) Spectroscopy, molecular; (300.6430) Spectroscopy, optoacoustic and thermo-optic; (140.3070) Infrared and far-infrared lasers; (140.3600) Lasers, tunable;

References and links

1. S. Blaser, D. Yarekha, L. Hvozdara, Y. Bonetti, A. Muller, M. Giovannini, and J. Faist, "Room-temperature, continuous-wave, single-mode quantum-cascade lasers at λ≈5.4 μm," Appl. Phys. Lett. **86**, 041109 (2005).
2. A. Evans, J. S. Yu, J. David, L. Doris, K. Mi, S. Slivken, and M. Razeghi, "High-temperature, high-power, continuous-wave operation of buried heterostructure quantum-cascade lasers," Appl. Phys. Lett. **84**, 314-316 (2004).
3. J. S. Yu, S. Slivken, A. Evans, S. R. Darvish, J. Nguyen, and M. Razeghi, "High-power λ~9.5 μm quantum-cascade lasers operating above room temperature in continuous-wave mode," Appl. Phys. Lett. **88**, 091113 (2006).
4. L. Diehl, D. Bour, S. Corzine, J. Zhu, G. Hofler, M. Loncar, M. Troccoli and Federico Capasso, "High-temperature continuous wave operation of strain-balanced quantum cascade lasers grown by metal organic vapor-phase epitaxy," Appl. Phys. Lett. **89**, 081101 (2006).
5. R. Maulini, A. Mohan, M. Giovannini, J. Faist, and E. Gini, "External cavity quantum-cascade lasers tunable from 8.2 to 10.4 um using a gain element with a heterogeneous cascade," Appl. Phys. Lett. **88**, 201113 (2006).
6. T. Aellen, S. Blaser, M. Beck, D. Hofstetter, J. Faist, and E. Gini, "Continuous-wave distributed-feedback quantum-cascade lasers on a Peltier cooler," Appl. Phys. Lett. **83**, 1929-1931 (2003).
7. G. Wysocki, R. F. Curl, F. K. Tittel, R. Maulini, J. M. Bulliard, and J. Faist, "Widely tunable mode-hop free external cavity quantum cascade laser for high resolution spectroscopic applications," Appl. Phys. B **81**, 769-777 (2005).
8. J. S. Yu, S. Slivken, S. R. Darvish, A. Evans, B. Gokden, and M. Razeghi, "High-power, room-temperature, and continuous-wave operation of distributed-feedback quantum-cascade lasers at λ~4.8 μm," Appl. Phys. Lett. **87**, 041104 (2005).
9. M. Pushkarsky, A. Tsekoun, I. G. Dunayevskiy, R. Go, and C. K. N. Patel, "Sub-parts-per-billion level detection of NO_2 using room-temperature quantum cascade lasers," Proc Natl. Acad. Sci. U S A. 2006 July 18; 103(29): 10846–10849

#82243 - $15.00 USD Received 19 Apr 2007; revised 24 May 2007; accepted 24 May 2007; published 31 May 2007

10. M. C. Phillips, T. L. Myers, M. D. Wojcik, and B. D. Cannon, "External cavity quantum cascade laser for quartz tuning fork photoacoustic spectroscopy of broad absorption features," Opt. Lett. **32**, 1177-1179 (2007).
11. L. Diehl, D. Bour, S. Corzine, J. Zhu, G. Hofler, M. Loncar, M. Troccoli and Federico Capasso, "High-power quantum cascade lasers grown by low-pressure metal organic vapor-phase epitaxy operating in continuous wave above 400 K," Appl. Phys. Lett. **88**, 201115 (2006).
12. A. A. Kosterev, Yu. A. Bakhirkin, R. F. Curl, and F. K. Tittel, "Quartz-enhanced photoacoustic spectroscopy," Opt. Lett. **27,** 1902-1904 (2002).
13. A. A. Kosterev, F. K. Tittel, D. Serebryakov, A. Malinovsky and A. Morozov, "Applications of quartz tuning fork in spectroscopic gas sensing," Rev. Sci. Instrum. **76**, 043105 (2005).
14. M. D. Wojcik, M. C. Phillips, B. D. Cannon, M. S. Taubman, "Gas-phase photoacoustic sensor at 8.41 μm using quartz tuning forks and amplitude-modulated quantum cascade lasers," Appl. Phys. B **85**, 307–313 (2006).
15. C. Y. Wang, L. Diehl, A. Gordon, C. Jirauschek, F. X. Kärtner, A. Belyanin, D. Bour, S. Corzine, G. Höfler, M. Troccoli, J. Faist, and F. Capasso, "Coherent instabilities in a semiconductor laser with fast gain recovery," Phys. Rev. A **75**, 031802(R) (2007).
16. G. Wysocki, *et.al* "High power continues wave broadly tunable external cavity quantum cascade laser operating at 8.4 μm for high resolution molecular spectroscopy," to be published.
17. R. Lewicki, G. Wysocki, A. A. Kosterev, and F. K. Tittel, "Carbon Dioxide and ammonia detection using 2μm diode laser based quartz-enhanced photoacoustic spectroscopy," Appl. Phys. B **87**, 157–162 (2007).
18. A. A. Kosterev, Y. A. Bakhirkin, F. K. Tittel, S. Blaser, Y. Bonetti, and L. Hvozdara, "Photoacoustic phase shift as a chemically selective spectroscopic parameter," Appl. Phys. B (Rapid Communications) **78**, 673-676 (2004).
19. R. D. Grober, J. Acimovic, J. Schuck, D. Hessman, P. J. Kindlemann, J. Hespanha, A. S. Morse, K. Karrai, I. Tiemann, and S. Manus, "Fundamental limits to force detection using quartz tuning forks," Rev. Sci. Instrum. **71**, 2776 (2000).
20. G. Wysocki, A. A. Kosterev, and F. K. Tittel, "Spectroscopic trace-gas sensor with rapidly scanned wavelengths of a pulsed quantum cascade laser for in situ NO monitoring of industrial exhaust systems," Appl. Phys. B **80**, 617-625 (2005).

1. Introduction

The recent progress in the development of quantum cascade lasers (QCLs) has led to the availability of robust mid-infrared spectroscopic light sources capable of high output power and room temperature operation [1-5]. QCLs cover the region from 3.7 to 20 μm where most molecules have fundamental absorption bands, which makes them useful for trace gas detection. For accurate spectroscopic analysis both single transverse and longitudinal mode operation for QCLs are required. The latter can be achieved by formation of a periodic structure within the QCL active region providing distributed feedback (DFB) for a single longitudinal laser mode at a precisely selected wavelength [6] or by using an external cavity configuration (EC) [7]. The tunability of DFB QCL relies on thermal tuning of the refractive index by temperature or injection current variation, which limits the frequency coverage to ~ 10 - 20 cm^{-1}. Furthermore, an increase of the QCL temperature during the tuning process results in a significant decrease of the output optical power. Therefore DFB-QCLs are typically designed for operation at a single target frequency with a practical tuning range of few wavenumbers (cm^{-1}) [8] and are usually used in trace gas detection and quantification of small molecules with narrow, resolved ro-vibrational lines. Such applications can also be realized using an EC-QCLs with mode-hop free tuning [7], or a quasi-continuous frequency tuning based on mode-hopping between closely spaced longitudinal modes of a very long external cavity [9]. For spectroscopic concentration measurements of broadband absorbing molecular species the EC-QCL source configuration is a preferred approach [10], mainly because of the much wider wavelength tuning range (>100cm^{-1}) which is primarily limited by the effective gain bandwidth of the QCL chip. In this work, a buried heterostructure MOVPE-grown QCL [11] operating in continuous wave at 8.4 μm in an EC configuration was used and a single mode tuning range of 135 $cm^{-1}$was achieved. The maximum available optical power of 50 mW (at a QCL heatsink temperature of -30°C) is sufficient for most spectroscopic applications, especially those that require single mode operation, narrow

#82243 - $15.00 USD Received 19 Apr 2007; revised 24 May 2007; accepted 24 May 2007; published 31 May 2007
(C) 2007 OSA

spectral linewidth, wavelength tunability and high optical power as for example in the detection and monitoring of several molecules simultaneously.

In this work a quartz enhanced photoacoustic spectroscopy (QEPAS) [12, 13] technique, which employs a quartz tuning fork (QTF) as an acoustic wave transducer was chosen for trace gas detection. QEPAS is well suited to applications that use broadly tunable sources because it is intrinsically wavelength insensitive and offers at the same time high sensitivity, compact size and immunity to environmental noise. In the case of broadband absorbers having non-resolved rotational-vibrational structure, the QEPAS signal is generated by modulating the laser radiation intensity. A similar approach employing an amplitude modulated (AM) 8.41 μm Fabry Perot (FP) QCL for QEPAS detection of Freon 134a was recently reported by Wojcik et al. [14]. However, the control of the FP-QCL wavelength is not straightforward. Furthermore, the width of the FP-QCL spectral envelope (as a result of multimode generation) strongly depends on the injection current and is also subject to instabilities [15]. Such a behavior would cause considerable uncertainties of the spectroscopic data. Precise frequency control can be achieved by application of the EC-QCL configuration as mentioned above.

2. Sensor configuration

A schematic diagram of the trace gas sensor platform is presented in Fig. 1. A EC-QCL in a Littrow configuration capable of providing single frequency radiation tunable between 1122 cm^{-1} and 1257 cm^{-1} is a significantly improved version of the system reported in Ref. [7]. Detailed description of the EC-QCL configuration and performance will be provided elsewhere [16]. A collimated laser beam (~15mm in diameter) is focused into a 320 μm wide gap between prongs of QTF using a 1-inch germanium lens (50 mm focal length). For broadly tunable systems the chromatic aberration of the used lenses starts to play an important role. The focal length scales as $1/(n\text{-}1)$, therefore the germanium with its high refractive index $n\approx4$ and negligible dispersion becomes the material of choice for a singlet lens material in the reported sensor configuration. To increase the sensitivity of QEPAS technique we mounted a metal tube (400 μm inner diameter and 2.45 mm long) on each side of the QTF, and these tubes act as an acoustic micro-resonator. The total length for the micro-resonator (5.2 mm including QTF thickness and gaps between QTF and both tubes) was selected to be equal to half acoustic wavelength at the frequency f=32.754 kHz, which corresponds to the resonant frequency of the QTF at a pressure of 770 Torr. Q-factor measured for the QTF at this pressure was $Q\approx10^4$. The absorption coefficient k of a species with unresolved absorption band scales linearly with pressure P up to very high pressures when pressure broadening becomes comparable to the width of absorption band (~40 cm^{-1} for Freon 125). The QEPAS signal S is proportional to kQ, and SNR~$kQ^{½}$ in the case of fast V-T relaxation. As established previously, $Q\sim P^{-½}$ in a first approximation [13]. Thus, both S and SNR are expected to increase with P. Indeed, such a growth for both S and the SNR was experimentally observed up to the highest pressure of 770 Torr allowed by our gas cell. Therefore, all the QEPAS experiments with the Freon 125 mixture were performed at a pressure of 770 Torr.

In case of background free QEPAS employing wavelength modulation (WM) technique the micro resonator provides usually an improvement of detection sensitivity by factor of ~7 [17]. WM-QEPAS can not be applied to concentration measurements of broadband absorbers. AM-QEPAS used in this work is in practice not a background free technique. Introduction of the micro-resonator caused further increase of that background, but still yielded a 3.5 times SNR improvement.

#82243 - $15.00 USD Received 19 Apr 2007; revised 24 May 2007; accepted 24 May 2007; published 31 May 2007
(C) 2007 OSA

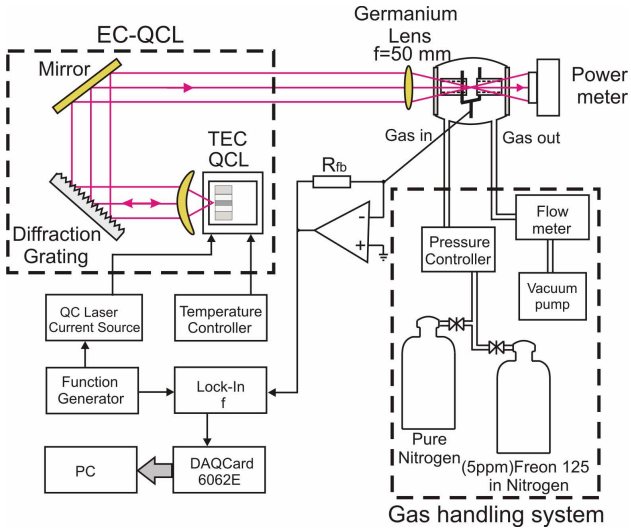

Fig. 1. Schematic diagram of the QEPAS based sensor platform with a CW EC-QCL spectroscopic source operating at 8.4 μm

The laser radiation exiting an absorption detection module (ADM), which consists of a QTF and micro-resonator enclosed in the sealed gas chamber, was directed to a power meter head for normalization purposes. The QCL was operated with an average current of 350 mA and 32.754 kHz square wave amplitude modulation of 600 mA peak-to-peak (50% duty cycle and 100% modulation depth of laser intensity). The average optical power of the laser radiation delivered to the ADM for these QCL operating conditions was 6.6 mW. The acoustically generated piezoelectric current in the QTF was converted to voltage by a custom built trans-impedance preamplifier and detected at the 1st harmonic frequency using a commercial lock-in amplifier (Signal Recovery Model 7265). An ILX Lightwave current source (Model LDX-3232) was used to power the QC laser, and the laser temperature was stabilized by a Wavelength Electronics temperature controller (Model MPT 10000). For all the measurements the temperature of the laser chip was kept constant at -30º C.

3. Experimental results

For a demonstration of the system performance, the spectroscopic measurements of Freon 125 (pentafluoroethane) absorption, which has two broad unresolved absorption bands within the tuning range of our EC-QCL, were carried out.

The EC-QCL frequency scan was performed using motorized coarse tuning of the diffraction grating angle. The calibration of the frequency scan was performed using both a 1/8 m monochromator as well as by means of a cross-comparison of the measured spectra with a molecular spectroscopic database. In all spectral measurements in this work the minimum incremental step of grating rotation was equal to 4.6×10^{-3} deg. This corresponds to an optical frequency change of 0.139 cm^{-1} calculated using the diffraction grating equation at 8.4 μm, which is the center wavelength of our EC-QCL. In a good approximation this corresponds to the spectral resolution of our instrument. Such an assumption can be made, because of the high quality AR coating (reflectivity of ~2×10^{-4}) deposited on the output facet of the QCL chip, which should efficiently suppress mode-hopping between the QCL modes separated by $FSR_{QCL}\approx0.5$ cm^{-1}. The influence of the mode-hopping between the longitudinal modes of the 8 cm long EC separated by a free spectral range of $FSR_{QCL}\approx0.0625$ cm^{-1}, which is smaller than 0.139 cm^{-1}, can also be neglected in this case.

#82243 - $15.00 USD Received 19 Apr 2007; revised 24 May 2007; accepted 24 May 2007; published 31 May 2007
(C) 2007 OSA

A calibrated reference mixture of 5 ppm of Freon 125 in nitrogen balance was used for these measurements. The laser wavelength was tuned from 1127 to 1245 cm^{-1} by means of a diffraction grating rotation, and for each selected spectral point both in-phase (X) and quadrature (Y) components of the QEPAS signal were measured and stored for post-processing. Unlike 2f wavelength modulation QEPAS, 1f AM QEPAS is not background free. Residual absorption of laser radiation by the cell windows as well as scattered radiation absorbed inside the gas cell produce a sound at the TF resonant frequency, thus generating a coherent background. However, we found this background to be stable over at least several hours, which permitted an efficient background subtraction. To determine the photoacoustic signal originating from the molecular absorption by the target gas, the background signal was separately measured with a pure N_2 and subsequently subtracted from the total signal measured for Freon 125. For every spectral point both components of the acquired signal (X_S,Y_S) and the background (X_B,Y_B) are normalized to the laser power recorded at the same time. In post-processing, the in-phase (X_{PA}) and the quadrature (Y_{PA}) components of the Freon-related photoacoustic signal were calculated as $X_{PA}=X_S-X_B$ and $Y_{PA}=Y_S-Y_B$ respectively. Vector subtraction was necessary because the phase of the background signal varied during a spectral scan. The reference frame for the data representation in Fig. 2 (that is, the in-phase X'_{PA} and quadrature Y'_{PA} projections of the signal) is selected in such a way that Y'_{PA} does not contain the Freon generated signal [18]. The resulting 1000 points spectrum of 5 ppm Freon 125 in N_2 mixture overlapped with a reference absorption spectrum obtained from the PNNL spectroscopic database is presented in Fig. 2. It can be seen that unlike the background signal, the Freon-generated PA signal has a constant phase over the entire spectral range. Excellent agreement of the measured spectrum with the database reference is evident and proves the feasibility of highly selective molecular identification. In order to estimate the measurement precision for our sensor platform as well as linearity of the AM-QEPAS signal versus the absorption coefficient, each X'_{PA} data point from the Fig. 2 spectrum (main plot) is mapped against the absorption coefficient determined at the same wavelength from the reference spectrum. The result is shown in Fig. 2 inset. The least squares linear fitting of the data yielded a correlation coefficient of R= 0.99886, which confirms the linear relation between the measured photoacoustic signal and the corresponding absorption coefficient. The slope of $a=2.827\times10^{-4}\ cm^{-1}\cdot W/V$ calculated with an accuracy of $\pm2.7\times10^{-7}\ cm^{-1}\cdot W/V$ can be used as the calibration coefficient of the photoacoustic signal. Based on the 5 ppm Freon 125 concentration in the calibrated gas mixture, a measurement precision of 4.5 ppb was determined.

#82243 - $15.00 USD Received 19 Apr 2007; revised 24 May 2007; accepted 24 May 2007; published 31 May 2007
(C) 2007 OSA

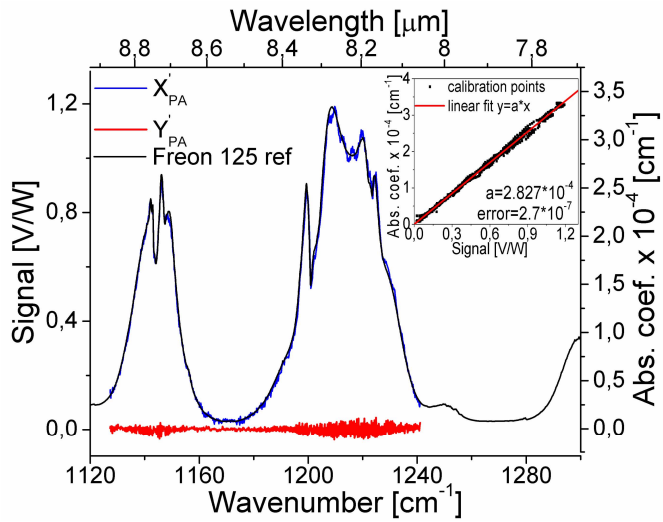

Fig. 2. An AM-QEPAS spectrum normalized to optical power recorded for a 5 ppm Freon 125 in N_2 mixture (the in phase X'_{PA} and quadrature Y'_{PA} components after rotation of the valence reference plane) fitted to the reference spectrum obtained from the PNNL database. The inset illustrates the calibration curve for absorption coefficient as a function of the photoacoustic signal.

A plot in Fig. 2 reveals several kinds of noise and background signals. A quadrature component while globally flat displays a fringe-like pattern with the amplitude clearly scaling with the Freon absorption. This is related to a photoacoustic signal resulting from Freon absorption of the stray light outside the microresonator. The in-phase signal is well fitted by the reference absorption spectrum but also shows fringe-like fluctuations proportional to the absorption coefficient. While such fluctuations related to laser and alignment instabilities impair the measurements accuracy, they do not impact the minimum detectable concentration limit (MDL). Furthermore, the fundamental thermal noise of the QTF is also present and primarily determines the MDL, as will be shown below.

To characterize the sensor performance without the laser tuning related instabilities, the optical laser frequency was fixed at 1208.62 cm^{-1}, which corresponds to the maximum Freon absorption within the EC-QCL tuning range. The average optical power between the QTF prongs was 6.6 mW (with the QCL operating in a 50% duty cycle), and the lock-in amplifier time constant was τ=1s with a 6 dB/oct low-pass filter. Figure 3 shows an example of the AM-QEPAS signal (in-phase component, as referred to the Freon 125 produced signal) when either the calibration mixture or pure nitrogen were flowing through the cell alternately. The response time to 90% of the steady-state signal is 10s with a <200 sccm flow rate. A MDL (1σ) of ~3ppb was calculated for these conditions based on the scatter of the background signal measurements. The normalized noise equivalent absorption coefficient (NNEA) of this sensor was determined to be $2.64 \times 10^{-9}\ W \cdot cm^{-1}/\sqrt{Hz}$ for Freon 125. Such a small NNEA value is an indication of the short V-T relaxation time τ in the system under study ($2\pi f<1/\tau$).

#82243 - $15.00 USD Received 19 Apr 2007; revised 24 May 2007; accepted 24 May 2007; published 31 May 2007
(C) 2007 OSA

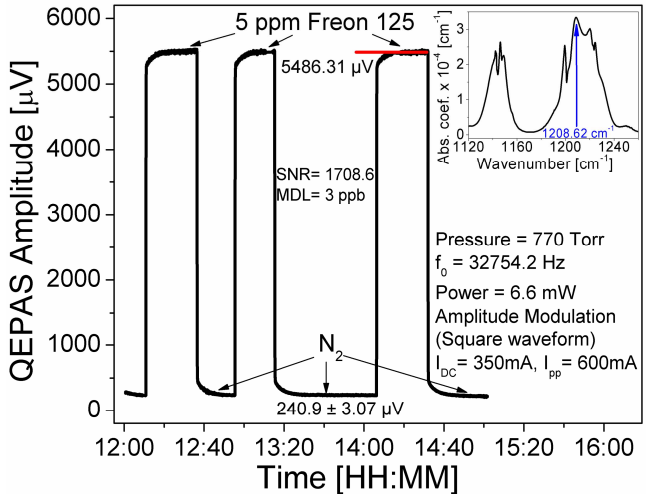

Fig. 3. Freon 125 concentration measurements performed with a tunable cw 8.4 μm EC-QCL based AM-QEPAS trace gas sensor system at 1208.62cm^{-1}. The inset depicts the spectral location of the laser frequency on the Freon 125 absorption spectrum accessible by the EC-QCL.

The noise level (1σ) of 3.07μV_{rms} observed for background measurement presented in Fig. 3 is primarily determined by fundamental thermal noise of the QTF [19]. The theoretical value of the thermal noise is $\sqrt{\Delta_N^2} \approx 1.9\mu V_{rms}$ calculated using $\frac{\sqrt{\Delta_N^2}}{\sqrt{\Delta f}} = R_g \sqrt{\frac{4 \cdot k_B T}{R}}$ equation, where R_g=10^7 Ω is the gain resistor in the transimpedance amplifier, T=297K, R=110 kΩ is the QTF equivalent dynamic resistance, Δf is the measurement bandwidth (0.25 Hz) and k_B is the Boltzmann constant. Allan variance analysis (Fig. 4) shows that the measurement accuracy improves with averaging time t, although slower than $t^{-0.5}$ which indicates a presence of the low-frequency noise input. For t=100s, the Allan deviation corresponds to the noise-equivalent concentration of 0.1 ppb. A scatter of the signal for 5 ppm Freon concentration is ~3.5 times higher, but it does not impact the MDL.

#82243 - $15.00 USD Received 19 Apr 2007; revised 24 May 2007; accepted 24 May 2007; published 31 May 2007
(C) 2007 OSA

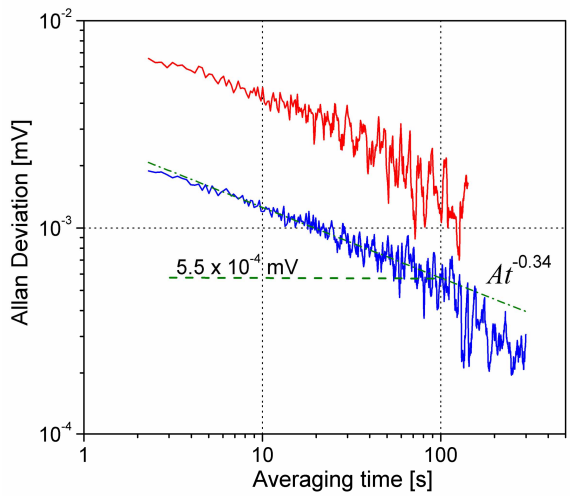

Fig. 4. Allan deviation (the square root of the Allan variance) calculated for the longest periods of steady Freon 125 concentrations in Fig. 3: red curve – 5 ppm Freon 125 in nitrogen, blue curve – pure nitrogen.

For comparison, an analysis of the MDL for the spectral measurements was also performed. Using the data acquired for pure nitrogen during two spectral scans separated by several hours (one as a background the second as a signal), the standard deviation calculated within the whole spectral range for one of the signal components yielded $1\sigma \sim 3.77 \mu V_{rms}$. A measurement precision of 1 ppb, which is essentially the MDL of the system, was determined by comparison with the Freon reference spectrum. The ~20% increase in the noise level in comparison to the noise determined for a single spectral point measurement indicates additional sources of noise and/or instabilities introduced by the spectral scan, such as spectral noise of the laser frequency affected by mode-hopping, or small changes in laser beam alignment (due to e.g. chromatic dispersion of the CaF_2 windows in the ADM or small changes in the laser beam quality).

To demonstrate an application of a broadly tunable EC-QCL for AM-QEPAS based multi-species detection a mixture of two absorbers, acetone and Freon 125, that have overlapped absorption spectra within the EC-QCL tuning range, was used. The system response to the acetone absorption was calibrated using a 8 ppm concentration of acetone in N_2 mixture obtained from a permeation based gas generator (Kin-Tek Model 491M) and a single spectral point measurement taken at the laser frequency corresponding to the maximum absorption coefficient of acetone within the tuning range (1217.7 cm^{-1}). For a 1 sec lock-in time constant and an effective optical power of 6.8 mW a MDL (1σ) of ~ 520 ppb was measured, which yielded a calibration coefficient of 1.53×10^{-3} $cm^{-1}\cdot W/V$. This value is 5.3 times higher than the one obtained for Freon, resulting in a lower QEPAS sensitivity to acetone. The difference of calibration coefficients for Freon 125 and acetone indicates different V-T energy relaxation pathways for these two molecules. The gas mixture containing both target species was prepared using liquid phase acetone placed in a cooling trap at a dry ice temperature (-78.5ºC) and flushing the trap with the reference mixture of 5 ppm Freon 125 in N_2. A sufficiently low partial pressure of acetone at this temperature produced a stable blend of Freon 125 and acetone within the dynamic range of our sensor system. A spectrum recorded for the gas mixture with an unknown concentration of both gases is shown in Fig. 5. Fitting this spectrum by a linear combination of separately acquired reference spectra of acetone and Freon 125, the concentrations of both species were retrieved from the measured composite spectrum. A spectrum measured for calibrated mixture of 5 ppm Freon 125 in N_2 was used as a reference

#82243 - $15.00 USD Received 19 Apr 2007; revised 24 May 2007; accepted 24 May 2007; published 31 May 2007
(C) 2007 OSA

spectrum for the Freon determination. The acetone concentration was calculated using a reference absorption spectrum obtained from the PNNL spectroscopic database and the previously determined QEPAS calibration coefficient for acetone. The calculated concentration of acetone and Freon in the custom gas mixture was found to be 47.2 ppm and 4.4 ppm, respectively. The acetone spectrum obtained as a result of subtraction of the Freon component from the net acquired spectrum perfectly coincided with the acetone spectrum from the FTIR database (see Fig. 5), giving an additional validation proof for this technique.

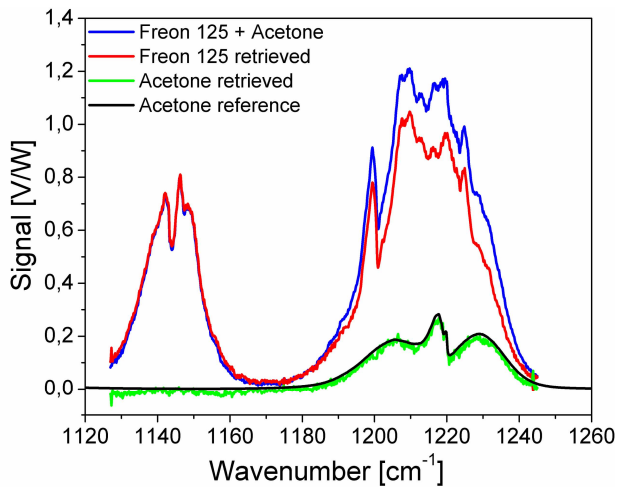

Fig. 5. AM-QEPAS spectrum of a Freon 125 and acetone mixture normalized to optical power plotted together with retrieved component spectra of Freon 125 (red line) and acetone (green line). The calculated acetone spectrum was fitted by a reference spectrum of acetone from the PNNL spectroscopic database shown as a black line.

4. Conclusions

In this work we demonstrated a high power, continuous wave EC-QCL tunable over a wide spectral range (135 cm^{-1}), which was applied to the detection of molecules with broadband unresolved ro-vibrational spectral structure. We observed an excellent agreement between measured photoacoustic spectra of Freon 125 and acetone in comparison to the reference data from a spectroscopic database. This demonstrates the feasibility of performing high sensitivity molecular spectroscopic measurements with detection limits at ppb-levels. The main limitations associated with the techniques presented in this paper are: 1) long data acquisition time for the measurements of a broad photoacoustic spectra, in which a time of 6 sec is required for an acquisition of a single spectral point (this is mainly limited by the acquisition time required for the lock-in detection of the QTF signal, which was performed with a measurement bandwidth of 0.25 Hz and requires a long settling time after each wavelength step) and 2) low specificity of a single spectral point measurement, which can be easily disturbed by any spectrally unspecific absorption in the system. Both issues will be addressed in the next phase of the instrument development by using a wide wavelength coverage but sampling only a few spectral points (similar to the method discussed in Ref. [20] to probe an absorption spectrum at the most informative, precisely selected optical frequencies. The system can be further improved by addressing other identified issues that will include: minimizing the photoacoustic background noise, improving the precision of the coarse wavelength tuning of the EC-QCL system, as well as improving the ADM design including the optimization of the acoustic micro resonator and a QTF with a higher conversion efficiency of the photoacoustic signal.

#82243 - $15.00 USD Received 19 Apr 2007; revised 24 May 2007; accepted 24 May 2007; published 31 May 2007
(C) 2007 OSA

Acknowledgments

The authors wish to thank Prof. Federico Capasso, Dr. Laurent Diehl and Dr. Mariano Troccoli for providing the QCL gain chip used for the reported studies, as well as Prof. Jerome Faist and Dr. Richard Maulini for an excellent AR coating applied to the QCL output facet. The authors acknowledge financial support from the MIRTHE NSF ERC, a subaward of a DoE STTR grant from Aerodyne Research, Inc, DARPA via a subaward from Pacific Northwest National Laboratory (PNNL) and the Robert Welch Foundation.

#82243 - $15.00 USD Received 19 Apr 2007; revised 24 May 2007; accepted 24 May 2007; published 31 May 2007
(C) 2007 OSA